

ImageBreed: Open-access plant breeding web–database for image-based phenotyping

Nicolas Morales¹  | Nicholas S. Kaczmar¹ | Nicholas Santantonio¹ | Michael A. Gore¹  | Lukas A. Mueller² | Kelly R. Robbins¹ 

¹Plant Breeding and Genetics Section, School of Integrative Plant Science, Cornell Univ., Ithaca, NY 14853, USA

²Boyce Thompson Institute, Ithaca, NY 14853, USA

Correspondence

Plant Breeding and Genetics Section, School of Integrative Plant Science, Cornell Univ., Ithaca, NY 14853, USA.
Email: krr73@cornell.edu

Funding information

NIFA USDA Hatch; Iowa Corn Promotion Board

Abstract

High-throughput image-phenotyping promises to accelerate the rate of genetic improvement in plant breeding through varietal selections informed by longitudinal growth models. To facilitate routine analyses and to drive breeding decisions, data integration is critical for effective management of germplasm, field experiment design, phenotyping, tissue sampling, genotyping, aerial-phenotyping campaigns, image files, and geo-spatial information. To this end, ImageBreed provides a software solution for end-to-end image-based phenotyping integrated into the Breedbase plant breeding system. ImageBreed provides open-source orthophotomosaic construction for raw image captures from standard color cameras and from the MicaSense Red-Edge multispectral camera. Additionally, previously assembled orthophotomosaic raster images can be uploaded. Orthophotomosaic images allow for streamlined extraction of plot-polygon images; however, ImageBreed plot-polygon images can also be extracted directly from raw aerial image captures. A web–database interface streamlines assignment of plot-polygon images from the orthophotomosaic or raw aerial-captures to the field experiment design. Image processes spanning Fourier-transform filtering, thresholding, and vegetation index masking are applied to reduce noise in extracted phenotypes. Summary-statistic phenotypic values are extracted for every observed plot-polygon image using a structured ontology. Plot-polygon images are queryable against genotypic, phenotypic, and experimental design information for training of machine learning models and

Abbreviations: API, application programming interface; CNN, convolutional neural network; FT-HPF, Fourier transform high-pass filter; FT-LPF, Fourier transform low-pass filter; ND, Chado Natural Diversity Database Schema; NDRE, normalized difference red-edge vegetation index; NDVI, normalized difference vegetation index; TGI, triangular greenness index; UAV, unoccupied aerial vehicle; VARI, visible atmospherically resistant index.

This is an open access article under the terms of the Creative Commons Attribution License, which permits use, distribution and reproduction in any medium, provided the original work is properly cited.

© 2020 The Authors. *The Plant Phenome Journal* published by Wiley Periodicals, Inc. on behalf of American Society of Agronomy and Crop Science Society of America.

for driving breeding decisions in varietal advancement. ImageBreed is publicly available at <http://imagebreed.org> and built on the open-source Breedbase system (<https://github.com/solgenomics/sgn>); all image-processing scripts are available at <https://github.com/solgenomics/DroneImageScripts> and via a Docker image. All data deposited in <http://imagebreed.org> are publicly available for longitudinal model training and for driving future breeding decisions.

1 | INTRODUCTION

The emergence of high-throughput aerial-phenotyping allows for near real-time evaluation of large numbers of genotypes, significantly impacting the field of plant phenomics (Ninomiya, Baret, & Cheng, 2019). Several studies have demonstrated the potential benefit of aerial-phenotyping in plant breeding across a range of crop species (Thorp, Thompson, Harders, French, & Ward, 2018; Krause, et al. 2019). However, routine use for breeding decisions requires rapid data turnaround and image processing remains a significant bottleneck in breeding programs.

Unoccupied aerial vehicles (UAVs) and occupied aircraft mounted with multispectral and color-image cameras now frequently fly over agricultural field experiments. For convenience in plot-polygon extraction, the raw image captures can be assembled into an orthophotomosaic image (American Society of Civil Engineers, 1994; Shi et al., 2016). Open-source software, such as the OpenCV computer-vision library, and commercial products are available to perform the orthophotomosaic assembly; however, these methods are either highly technical or expensive (Bradski, 2000; Culjak, Abram, Pribanic, Dzapov, & Cifrek, 2012; Rublee, Rabaud, Konolige, & Bradski, 2011). Alternatively, ImageBreed performs orthophotomosaic assembly in a free, streamlined interface designed for phenotypic value extraction in the context of plant breeding. Furthermore, ImageBreed allows researchers to bypass orthophotomosaic assembly in order to extract plot-polygons directly from raw aerial image captures. Figure 1 provides an overview of the primary dashboard interface. A user guide for Breedbase is available at <https://solgenomics.github.io/sgn/> with information regarding ImageBreed in the “Managing Image Data for Phenotyping” section in the supplemental information.

2 | MATERIALS AND METHODS

ImageBreed is implemented within the codebase of Breedbase, which is an open-source web-database for managing germplasm, field experiment design, tissue sampling,

phenotypic, and genotypic information; it is currently used by many plant breeding communities, including <https://cassavabase.org> and <https://solgenomics.net> (Fernandez-Pozo, Menda, & Edwards, 2014). Breedbase employs the Chado database schema, the Natural Diversity (ND) module, and controlled vocabulary driven data models, allowing for a highly extensible system (Jung et al., 2011; Mungall, Emmert, & The FlyBase Consortium, 2007). Figure 2 presents the primary relational database schema. Ontologies are used for annotating phenotypic values and images within Breedbase (Shrestha et al., 2012). The supplemental information contains the image-phenotyping ontologies.

Breedbase, and subsequently ImageBreed, is written in Perl and connects to a PostgreSQL database; the software is open source (<https://github.com/solgenomics/sgn>). Development of Breedbase is ongoing and uses Github as a repository for tracking issues and new features. RESTful endpoints are constructed using the Catalyst web-framework and constitute the primary means of communication between Breedbase’s JavaScript based web-interface and the database. The supplemental information contains the complete ImageBreed web-application programming interface (API) specification. All image processes are performed using Python scripts that interface with the OpenCV library (<https://github.com/opencv/opencv>); MicaSense open-source scripts are used for orthophotomosaic assembly of RedEdge camera 5-band multispectral captures (<https://github.com/micasense/imageprocessing>). The image-processing scripts are available with a Docker image for standalone use (<https://github.com/solgenomics/DroneImageScripts>).

2.1 | Field experiments

Prior to processing aerial images, the field experiment must first be saved in the database. The field experiment represents the design with which accessions are distributed among experimental field plots in a given field location. More information on field experiments is available in the Breedbase documentation (<https://solgenomics.github.io/sgn/>) in the “Managing Field Trials” section. Importantly, Breedbase supports the Plant Breeding API (BrAPI) standard for

representing field experiments and associated metadata including phenotypic records (Selby et al., 2019). Once the field experiment is saved, aerial imaging campaigns can be uploaded for the field experiment and then plot-polygon images can be associated with their respective field experiment plots.

2.2 | Image input

The starting point in ImageBreed is either (a) upload of raw image captures (.tiff) from standard color cameras or from the Micasense Rededge 5-band multispectral camera, or (b) upload of previously stitched raster images (.PNG, .JPG). When starting with raw image captures, a compressed (.zip) archive is uploaded; the maximum upload size is currently 2 GB. Depending on user input, the raw image captures are assembled into an orthophotomosaic and saved as a PNG raster image or the raw image captures are saved as PNG images and used directly for plot-polygon assignment. The use of previously stitched raster images facilitates use of any camera instrument, granted the image is smaller than 1 GB and meets the spectral category conditions defined below.

Imaging campaigns are saved and denoted by spectral type as either blue (450–520 nm), green (515–600 nm), red (600–690 nm), red-edge (690–750 nm), near-infrared (NIR) (780–3,000 nm), mid-infrared (MIR) (3,000–50,000 nm), far-infrared (FIR) (50,000–1,000,000 nm), or thermal-infrared (thermal IR) (9,000–14,000 nm) (Iso, 2007). If the image spectrum is not known precisely, options exist for black-and-white or RGB color image. Each spectral category should only be used once in a given aerial imaging campaign; for example, when uploading imaging campaigns for the MicaSense Red-edge 5-band camera, the images should be uniquely tagged as blue, green, red, red-edge, and near-infrared. In addition to assigning a spectral category, users must provide a name and a description for each uploaded imaging campaign. As the system matures, it is expected this information can be automatically extracted from the uploaded image headers to facilitate the upload process. Note that uploading several previously stitched orthophotomosaic image bands requires that the bands are perfectly superimposable and of equal size; orthophotomosaic stitching software generally accomplishes this by default.

2.3 | Image processing

Noise in aerial-phenotyping imagery can stem from the camera and environmental conditions. To minimize camera and software-induced white noise, ImageBreed applies non-local means denoising (Buades, Coll, & Morel, 2011). In signal processing, the Fourier transform (FT) can remove noise

Core Ideas

- A pipeline for phenotype extraction from aerial images in agricultural experiments.
- ImageBreed's web-database interface allows for data standardization and sharing.
- Ontology based phenotype and image annotation allows for stable data representation.
- Breedbase stores aerial images alongside experimental phenotypic and genotypic data.
- Open-source orthophotomosaic construction for multispectral and standard imagery.

via high-pass filters (FT-HPF) or low-pass filters (FT-LPF) (Shaikh, Choudhry, & Wadhvani, 2016). ImageBreed performs FT-HPF to remove the lowest 20, 30, and 40 frequencies from images. ImageBreed performs magnitude thresholding on the high and low tails of the pixel distribution to remove noise pixels from images (Pandian, Ciulla, Mark Haacke, Jiang, & Ayaz, 2008). Furthermore, ImageBreed minimizes background soil pixels present in plot-polygon images by applying the following vegetation indices (VIs) as masks: normalized difference vegetation index (NDVI), triangular greenness index (TGI), visible atmospherically resistant index (VARI), and normalized difference red-edge vegetation index (NDRE) (Hunt et al., 2013; Robinson et al., 2017). Custom VIs, such as the soil-adjusted vegetation index (SAVI) (Huete, 1988), can be modularly added in the source code. All images are annotated using controlled vocabularies to account for the specific combination of processes applied.

Application of denoising, thresholding, FT-HPF, and VI calculation for a 5,000 × 6,000 pixel orthophotomosaic image containing 500 experimental field plots takes approximately 2 min on an E5-2660v2 2.2 GHz workstation with a Quadro K5000 GPU and 256 GB RAM; however, plot-polygon processing can take approximately 30 min to complete. Plot-polygon processing crops and saves individual plot-images for all uploaded image bands to ensure fast queries during downstream analyses. The hardware specifications above are used to run the public ImageBreed instance <http://imagebreed.org> locally; however, a GPU is not required, and a minimum of 8 GB RAM ensures performant functionality. Disk storage space is required for the database, saved images, and archived files; storage requirements are dependent on the scale of the project.

2.4 | Phenotype extraction

Extraction of phenotypic values from aerial imagery relies on assigning geo-spatial plot-polygons to each plot in the

The screenshot displays the ImageBreed web interface. At the top, there are navigation tabs: 'Upload Imagery', 'Download Image-Phenotypes', 'Keras CNN Models', 'Calculate Statistics', and 'Compare Aerial Field Images'. The main content area is divided into several sections:

- 1:** The 'Upload Imagery' button and its associated options.
- 2:** A list of field trials and imaging campaigns, with two campaigns highlighted: '2017_NYH2_06122017' and '2017_NYH2_08172017'.
- 3:** A 'Create Template' button for the selected campaign.
- 4:** An expanded view of the '2017_NYH2_08172017' campaign showing detailed metadata such as 'Imaging Event Name', 'Imaging Event Type', 'Description', 'Date', 'Averaged Temperature', 'Growing Degree Days', and 'Field Trial'.
- 5:** A section for 'View Plot Images Summary (2000)' showing a grid of image thumbnails.
- 6:** A section for 'View Images' showing a list of processed images with their respective dates and times.
- 7:** A section for 'NIR Image(s)' showing a grid of 500 plot polygons and a corresponding grid of 500 thresholded NIR plot-polygon images.
- 8:** A 'Delete Imaging Event' button.

FIGURE 1 ImageBreed Dashboard Overview. (1) Upload raw image captures in a compressed file (.zip) for use of the raw image captures directly or for orthophotomosaic assembly, or upload previously stitched raster orthophotomosaic imagery. Expanded window shows all aerial image actions. (2) Dashboard shows all field trials and uploaded imaging campaigns in collapsible sections. Two imaging campaigns, 2017_NYH2_06122017 and 2017_NYH2_08172017, are shown for the 2017_NYH2 field experiment of maize hybrids. (3) Follow standard processes to manually create templates for assignment of plot-polygon images to the field experiment design. Blue button is shown only when the standard process has not yet been completed. (4) Expanded window showing the 2017_NYH2_08172017 imaging event with its metadata including days after planting and growing degree days. (5) Uploaded multispectral image bands are displayed under the imaging event in collapsible sections. Shown is an image band tagged as near-infrared (780–3000 nm). All shown images originate from this uploaded image band. (6) Resulting images from standard process rotation and cropping of the relevant field from the uploaded image band are listed in display. (7) Resulting plot-polygon images from standard process are shown within collapsible sections. Highlighting 500 NIR plot-polygon images in an expanded window. Also shown are 500 thresholded NIR plot-polygon images. (8) Export phenotypic values from plot-polygon images for analyses and model training. Current and future ImageBreed features provide prediction of end-of-season traits with statistical and machine learning models

field experiment design. The assigned plot-polygons are generally square-rectangles of equal size and shape for all experimental field plots. Software such as QGIS can create plot-polygon representations (Andrade-Sanchez et al., 2014; QGIS Development Team 2017); however, ImageBreed provides a standardized, manual interface for performing the plot-polygon assignment by clicking the four corners of the field experiment and minimally specifying the number of experimental plot grid rows and columns. ImageBreed makes no assumptions on whether the uploaded raw image captures or orthophotomosaic are georeferenced in an effort to be as flexible as possible. Future work will allow previously used plot-polygon templates to be rescaled and applied onto new aerial imaging campaigns through a point and click interface. ImageBreed provides point and click functions

for copy-pasting plot-polygon templates and for removing specific polygons from consideration, allowing flexibility for templating even the most irregularly oriented field layouts. Plot-polygon images are then cropped out from the orthophotomosaic, annotated with the type of image and process applied, and stored as an entry in a relational database with association to the respective experimental plot in the field design and with association to the originating aerial-phenotyping event. For a detailed walk-through please consult the “Managing Image Data for Phenotyping” section in the Breedbase documentation <https://solgenomics.github.io/sgn> or consult the supplemental information.

ImageBreed extracts and annotates phenotypic values from plot-polygon images using ontologies. Table 1 summarizes the extracted phenotypic traits and image processes applied;

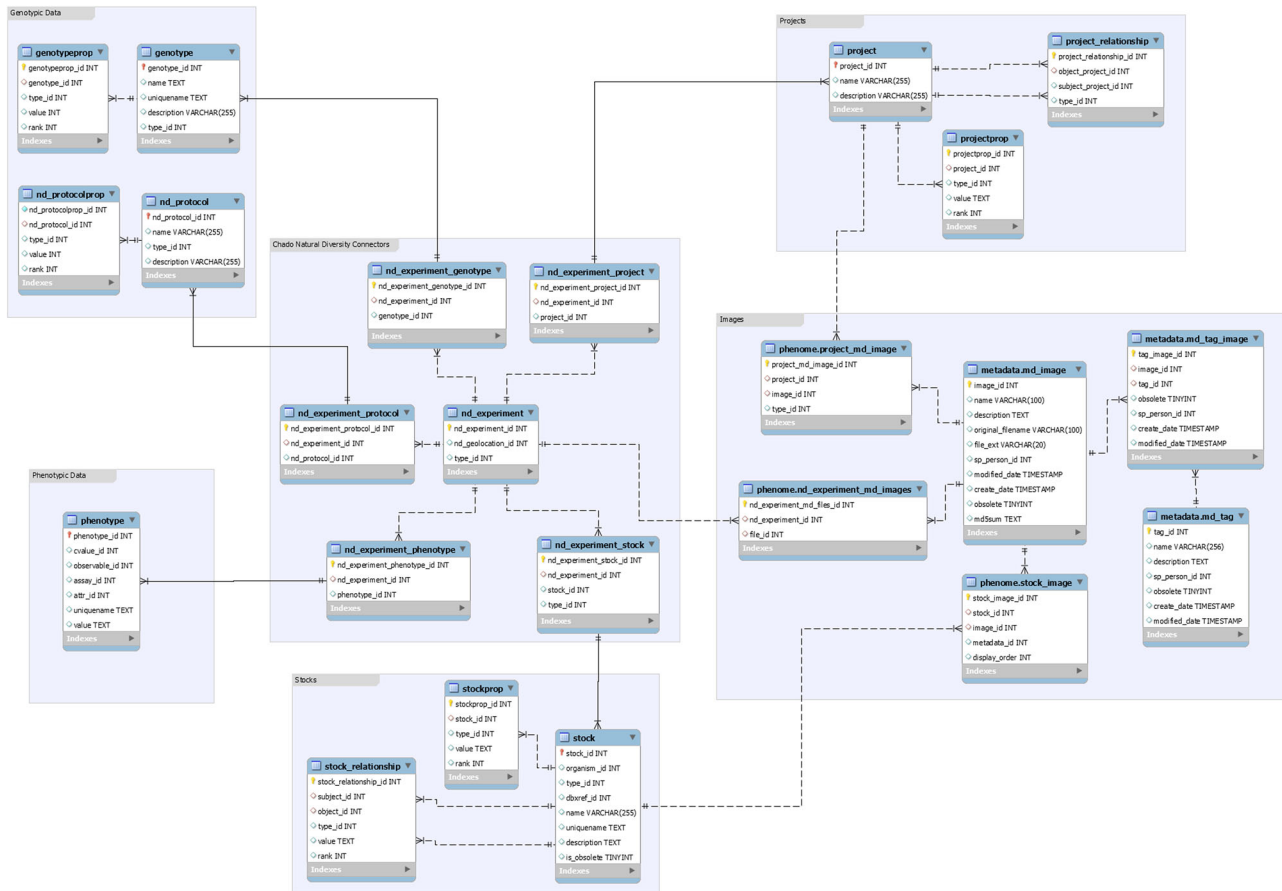


FIGURE 2 Relational database schema of Breedbase as used by ImageBreed. The schema can be divided into the following subdivisions: genotyping, phenotyping, stocks, projects, and images, with connector tables from the Natural Diversity (ND) module of the Chado database. Note that image files are stored in the file system and only filenames and metadata are stored in the database

furthermore, the supplemental information contains the complete image-phenotyping ontologies. Note that in Breedbase phenotypic annotations can be composed as combinations of ontologies; for instance, ‘Mean Pixel Value|NIR (780–3,000 nm)|NIR Denoised Original Image|day 105’ is a phenotypic annotation describing a mean pixel value from an original NIR image taken 105 d after planting. Composing annotations in this way ensures uniqueness and queriability of phenotypic values in the database. All plot-polygon images and phenotypic values stored within ImageBreed are public domain, allowing researchers to download and build upon existing datasets; currently <http://imagebreed.org> contains more than 500,000 plot-polygon images of maize (*Zea mays* L.) and barley (*Hordeum vulgare* L.). Aggregated data allows for training predictive longitudinal growth models across crop species and field environments, driving

breeding decisions in varietal advancement (van Eeuwijk et al., 2019; Xavier, Hall, Hearst, Cherkauer, & Rainey, 2017). Current and future work is focused on developing pipelines for training models to predict end-of-season traits from plot-level images, extracted phenotypes, and genetic relationships in Breedbase. Both longitudinal linear models and convolutional neural networks (CNNs) in Keras TensorFlow 2.0 are currently being developed.

SOFTWARE AVAILABILITY

ImageBreed is publicly available at <http://imagebreed.org> and built on the open-source Breedbase system (<https://github.com/solgenomics/sgn>); all image processing scripts are available at <https://github.com/solgenomics/DroneImageScripts> and via a Docker image.

TABLE 1 List of image processes applied to each plot-polygon image as well as a list of the extracted phenotypic values that ImageBreed currently supports. Phenotype annotations are composed as combinations of these ontologies; for instance, ‘Mean Pixel ValueNIR (780–3,000 nm)NIR Denoised Original ImageDay 105’ is a phenotypic annotation describing a mean pixel value from a denoised original NIR image taken 105 d after planting. In this way the annotations ensure uniqueness and queriability across the database. Consult the supplemental information for the complete ontologies used

| Processes for phenotype extraction | Methods and traits for phenotype extraction |
|------------------------------------|--|
| Image processes applied | Non-local means denoising Fourier-transform high pass filtering of lowest 20 frequencies Fourier-transform high pass filtering of lowest 30 frequencies Fourier-transform high pass filtering of lowest 40 frequencies Magnitude thresholding highest and lowest pixel values NDVI threshold masking NDRE threshold masking TGI threshold masking VARI threshold masking |
| Extracted phenotypic traits | mean pixel value total pixel sum number of non-zero pixels harmonic mean pixel value median pixel value pixel variance minimum pixel value maximum pixel value minority pixel value minority pixel count majority pixel value majority pixel count pixel group count |

Note. NDRE, normalized difference red-edge vegetation index; NDVI, normalized difference vegetation index; NIR, near-infrared; TGI, triangular greenness index; VARI, visible atmospherically resistant index.

CONFLICT OF INTEREST

The authors declare no conflicts of interest.

ACKNOWLEDGMENTS

This material is based upon work supported by the National Institute of Food and Agriculture, USDA, Hatch under 100397 (M.A.G.), 1010428 (M.A.G.), 1013637 (M.A.G.), 1013641 (M.A.G.), Iowa Corn, and Cornell University startup funds (M.A.G. and K.R.R.). We also acknowledge the contributions from Nicholas Lepak, Joshua Budka, Cinta Romay, and other current and past members of the Gore, Buckler, Smith, and Nelson labs. Additionally, we thank Kelly R. Thorp and Anna van Doorn for useful discussions, and Mahlet T. Anche and Karl Kunze for independent validation of the pipeline in their pre-publication maize and barley research endeavors, respectively.

ORCID

Nicolas Morales  <https://orcid.org/0000-0002-3600-0657>

Michael A. Gore  <https://orcid.org/0000-0001-6896-8024>

Kelly R. Robbins  <https://orcid.org/0000-0001-9522-9585>

REFERENCES

- American Society of Civil Engineers. (1994). *Glossary of the mapping sciences*. Reston, VA: ASCE.
- Andrade-Sanchez, P., Gore, M. A., Heun, J. T., Thorp, K. R., Carmo-Silva, A. E., French, A. N., ... White, J. W. (2014). Development and evaluation of a field-based high-throughput phenotyping platform. *Functional Plant Biology*, *41*(1), 68–79. <https://doi.org/10.1071/FP13126>
- Bradski, G. (2000) The opencv library. *Dr. Dobb's Journal of Software Tools*, *120*, 122–125.
- Buades, A., Coll, B., & Morel, J. M. (2011). Non-local means denoising. *Image Processing On Line*, *1*, 208–212. https://doi.org/10.5201/ipol.2011.bcm_nlm

- Culjak, I., Abram, D., Pribanic, T., Dzapo, H., & Cifrek, M. (2012). A brief introduction to OpenCV. In *2012 Proceedings of the 35th International Convention MIPRO, 21–25 May, Opatija, Croatia* (pp. 1725–1730). New York: IEEE.
- Fernandez-Pozo, N., Menda, N., & Edwards, J. D. (2014). The Sol Genomics Network (SGN)—from genotype to phenotype to breeding. *Nucleic Acids*, *43*, 1036–1041. <https://doi.org/10.1093/nar/gku1195>
- Huete, A. R. (1988). A soil-adjusted vegetation index (SAVI). *Remote Sensing of Environment*, *25*(3), 295–309. [https://doi.org/10.1016/0034-4257\(88\)90106-X](https://doi.org/10.1016/0034-4257(88)90106-X)
- Hunt, E. R., Doraiswamy, P. C., McMurtrey, J. E., Daughtry, C. S. T., Perry, E. M., & Akhmedov, B. (2013). A visible band index for remote sensing leaf chlorophyll content at the canopy scale. *International Journal of Applied Earth Observation and Geoinformation*, *21*(April), 103–112. <https://doi.org/10.1016/j.jag.2012.07.020>
- Iso, B. (2007). 20473: 2007 Optics and photonics. *Spectral Bands*, *10*, 3.
- Jung, S., Menda, N., Redmond, S., Buels, R. M., Friesen, M., Bendana, Y., ... Main, D. (2011). The Chado Natural Diversity Module: A new generic database schema for large-scale phenotyping and genotyping data. *Database: The Journal of Biological Databases and Curation*, *2011*(November), bar051.
- Krause, M. R., González-Pérez, L., Crossa, J., Pérez-Rodríguez, P., Montesinos-López, O., Singh, R. P., ... Mondal, S. 2019. Hyperspectral reflectance-derived relationship matrices for genomic prediction of grain yield in wheat. *Genes Genomes Genetics*, *9*(4), 1231–1247.
- Mungall, C. J., Emmert, D. B., & The FlyBase Consortium. (2007). A chado case study: An ontology-based modular schema for representing genome-associated biological information. *Bioinformatics*, *23*(13), i337–i346. <https://doi.org/10.1093/bioinformatics/btm189>
- Ninomiya, S., Baret, F., & Cheng, Z. M. (2019). Plant phenomics: Emerging transdisciplinary science. *Plant Phenomics*, *2019*(January), 2765120. <https://doi.org/10.34133/2019/2765120>
- Pandian, D. S. J., Ciulla, C., Haacke, E. M., Jiang, J., & Ayaz, M. (2008). Complex threshold method for identifying pixels that contain predominantly noise in magnetic resonance images. *Journal of Magnetic Resonance Imaging*, *28*(3), 727–735. <https://doi.org/10.1002/jmri.21487>
- QGIS Development Team. (2017). QGIS: A free and open source geographic information system. Retrieved from <https://qgis.org/en/site>
- Robinson, N. P., Allred, B. W., Jones, M. O., Moreno, A., Kimball, J. S., Naugle, D. E., ... Richardson, A. D. (2017). A dynamic landsat derived normalized difference vegetation index (NDVI) product for the conterminous united states. *Remote Sensing*, *9*(8), 863. <https://doi.org/10.3390/rs9080863>
- Ruble, E., Rabaud, V., Konolige, K., & Bradski, G. R. (2011). ORB: An efficient alternative to SIFT or SURF. *2011 International Conference on Computer Vision, Barcelona* (pp. 2564–2571). <https://doi.org/10.1109/ICCV.2011.6126544>
- Selby, P., Abbeloos, R., Backlund, J. E., Salido, M. B., Bauchet, G., Benites-Alfaro, O. E., ... Verouden, M. (2019). BrAPI—an application programming interface for plant breeding applications. *Bioinformatics*, *35*(20), 4147–4155. <https://doi.org/10.1093/bioinformatics/btz190>
- Shaikh, M. S., Choudhry, A., & Wadhvani, R. (2016). Analysis of digital image filters in frequency domain. *International Journal of Computer Applications in Technology*, *140*, 6. <https://doi.org/10.5120/ijca2016910836>
- Shi, Y., Thomasson, J. A., Murray, S. C., Pugh, N. A., Rooney, W. L., Shafian, S., ... Yang, C. (2016). Unmanned aerial vehicles for high-throughput phenotyping and agronomic research. *PLOS ONE*, *11*(7), e0159781. <https://doi.org/10.1371/journal.pone.0159781>
- Shrestha, R., Matteis, L., Skofic, M., Portugal, A., McLaren, G., Hyman, G., & Arnaud, E. (2012). Bridging the phenotypic and genetic data useful for integrated breeding through a data annotation using the crop ontology developed by the crop communities of practice. *Frontiers in Physiology*, *3*, 326. <https://doi.org/10.3389/fphys.2012.00326>
- Thorp, K. R., Thompson, A. L., Harders, S. J., French, A. N., & Ward, R. W. (2018). High-throughput phenotyping of crop water use efficiency via multispectral drone imagery and a daily soil water balance model. *Remote Sensing*, *10*(11), 1682. <https://doi.org/10.3390/rs10111682>
- van Eeuwijk, F. A., Bustos-Korts, D., Millet, E. J., Boer, M. P., Kruijer, W., Thompson, A., ... Champman, S. C. (2019). Modelling strategies for assessing and increasing the effectiveness of new phenotyping techniques in plant breeding. *Plant Science: An International Journal of Experimental Plant Biology*, *282*(May), 23–39. <https://doi.org/10.1016/j.plantsci.2018.06.018>
- Xavier, A., Hall, B., Hearst, A. A., Cherkauer, K. A., & Rainey, K. M. (2017). Genetic architecture of phenomic-enabled canopy coverage in *glycine max*. *Genetics*, *206*(2), 1081–1089. <https://doi.org/10.1534/genetics.116.198713>

SUPPORTING INFORMATION

Additional supporting information may be found online in the Supporting Information section at the end of the article.

How to cite this article: Morales N, Kaczmar NS, Santantonio N, Gore MA, Mueller LA, Robbins KR. ImageBreed: Open-access plant breeding web-database for image-based phenotyping. *Plant Phenome J.* 2020;3:e20004. <https://doi.org/10.1002/ppj2.20004>